Inositol pyrophosphates inhibit synaptotagmin-dependent exocytosis

Tae-Sun Lee[a,b,c,1], Joo-Young Lee[d,1], Jae Won Kyung[e], Yoosoo Yang[f], Seung Ju Park[d], Seulgi Lee[d], Igor Pavlovic[g], Byoungjae Kong[h], Yong Seok Jho[i], Henning J. Jessen[j], Dae-Hyuk Kweon[h], Yeon-Kyun Shin[k], Sung Hyun Kim[e,l,2], Tae-Young Yoon[b,c,2], and Seyun Kim[d,m,2]

[a]Department of Physics, Korea Advanced Institute of Science and Technology, Daejeon 34141, Korea; [b]Center for Nanomedicine, Institute for Basic Science (IBS), Yonsei University, Seoul 30722, Korea; [c]Yonsei-IBS Institute, Yonsei University, Seoul 30722, Korea; [d]Department of Biological Sciences, Korea Advanced Institute of Science and Technology, Daejeon 34141, Korea; [e]Department of Biomedical Science, Graduate School, Kyung Hee University, Seoul 02447, Korea; [f]Biomedical Research Institute, Korea Institute of Science and Technology, Seoul 02792, Korea; [g]Department of Chemistry, University of Zurich, 8057 Zurich, Switzerland; [h]Department of Genetic Engineering and Center for Human Interface Nanotechnology, Sungkyunkwan University, Suwon 16419, Korea; [i]Asia-Pacific Center for Theoretical Physics, Pohang, Gyeongbuk 37673, Korea; [j]Institute of Organic Chemistry, Albert-Ludwigs-University Freiburg, Freiburg 79104, Germany; [k]Department of Biochemistry, Biophysics, and Molecular Biology, Iowa State University, Ames, IA 50011; [l]Department of Physiology, School of Medicine, Neurodegeneration Control Research Center, Kyung Hee University, Seoul 02447, Korea; and [m]Korea Advanced Institute of Science and Technology Institute for the BioCentury, Korea Advanced Institute of Science and Technology, Daejeon 34141, Korea

Edited by Tomas G. M. Hokfelt, Karolinska Institutet, Stockholm, Sweden, and approved June 1, 2016 (received for review November 3, 2015)

Inositol pyrophosphates such as 5-diphosphoinositol pentakisphosphate (5-IP$_7$) are highly energetic inositol metabolites containing phosphoanhydride bonds. Although inositol pyrophosphates are known to regulate various biological events, including growth, survival, and metabolism, the molecular sites of 5-IP$_7$ action in vesicle trafficking have remained largely elusive. We report here that elevated 5-IP$_7$ levels, caused by overexpression of inositol hexakisphosphate (IP$_6$) kinase 1 (IP6K1), suppressed depolarization-induced neurotransmitter release from PC12 cells. Conversely, IP6K1 depletion decreased intracellular 5-IP$_7$ concentrations, leading to increased neurotransmitter release. Consistently, knockdown of IP6K1 in cultured hippocampal neurons augmented action potential-driven synaptic vesicle exocytosis at synapses. Using a FRET-based in vitro vesicle fusion assay, we found that 5-IP$_7$, but not 1-IP$_7$, exhibited significantly higher inhibitory activity toward synaptic vesicle exocytosis than IP$_6$. Synaptotagmin 1 (Syt1), a Ca^{2+} sensor essential for synaptic membrane fusion, was identified as a molecular target of 5-IP$_7$. Notably, 5-IP$_7$ showed a 45-fold higher binding affinity for Syt1 compared with IP$_6$. In addition, 5-IP$_7$–dependent inhibition of synaptic vesicle fusion was abolished by increasing Ca^{2+} levels. Thus, 5-IP$_7$ appears to act through Syt1 binding to interfere with the fusogenic activity of Ca^{2+}. These findings reveal a role of 5-IP$_7$ as a potent inhibitor of Syt1 in controlling the synaptic exocytotic pathway and expand our understanding of the signaling mechanisms of inositol pyrophosphates.

inositol pyrophosphate | synaptotagmin | synaptic vesicle exocytosis

Inositol phosphates (IPs) exist in all types of organisms from yeast to mammals. Inositol 1,4,5-trisphosphate (IP$_3$) is a well-known second messenger that elevates cytosolic Ca^{2+} levels through direct binding and activation of IP$_3$-gated Ca^{2+} channels (1). Recently, inositol pyrophosphates with highly energetic pyrophosphate bonds have been reported (2). In mammals, the most extensively characterized inositol pyrophosphate is 5-diphosphoinositol pentakisphosphate (5-PP-[1,2,3,4,6]IP$_5$), designated 5-IP$_7$. The 5-IP$_7$ is synthesized by phosphorylation at position 5 of the fully phosphorylated six-carbon inositol, inositol hexakisphosphate (IP$_6$) (3). Another IP$_7$ isomer, 1/3-PP-IP$_5$ (1-IP$_7$), influences phosphate homeostasis in yeast by binding to the cyclin/cyclin-dependent kinase complex and inactivating its function (3–5). The significant role of IP$_7$ in coordinating growth and metabolism of mammalian cells has been highlighted (6, 7). Mechanistically, IP$_7$ appears to signal through either covalent modification of proteins through phosphotransfer reactions (8) or allosteric interactions with specific receptor proteins (6). With few exceptions, such as Akt/PKB, which is inhibited when bound to 5-IP$_7$ (6, 9), the proteins that are directly targeted by IP$_7$ and the mechanism by which IP$_7$ allosterically modulates target protein function remain largely unknown.

Exocytosis is a key form of cell–cell communication, as represented by neurotransmitter release. This fundamental process is orchestrated by a group of proteins that includes soluble *N*-ethylmaleimide-sensitive factor attachment protein receptors (SNAREs) and synaptotagmin (Syt) (10–15). Once influx of Ca^{2+} occurs at the presynaptic terminal, Ca^{2+}-bound Syt1 governs vesicle fusion through macromolecular interactions with lipid membranes as well as SNARE proteins (11, 13–15). Since the early 1990s, IPs have been recognized as Syt-binding metabolites that down-regulate synaptic exocytosis, but their weak binding affinities for Syt and a lack of mechanistic understanding have cast doubt on their physiological relevance (16–19). Recently, IP$_6$ was also shown to suppress excitatory neurotransmission by inhibiting the presynaptic Syt1–C2B domain (20). In contrast, a study by Luo et al. proposed that IP$_6$ kinase 1 (IP6K1), which is responsible for 5-IP$_7$ synthesis, promotes synaptic vesicle exocytosis in a 5-IP$_7$–independent manner through direct protein–protein interactions between IP6K1 and guanine nucleotide exchange factor for Rab3A (GRAB) (21).

Given the unique chemical configuration of the IP$_7$ structure, the dynamic turnover of cellular IP$_7$ levels (9, 22–25), and implications

Significance

Inositol phosphates have long been considered to be negative regulators of synaptic exocytosis, but the function of diphosphoinositol pentakisphosphate (IP$_7$) has remained elusive. We found that overexpression and depletion of inositol hexakisphosphate (IP$_6$) kinase in PC12 cells or hippocampal neurons led to a reduction and increase in neurotransmitter release, respectively. Biophysical assays revealed that 5-IP$_7$ inhibited Ca^{2+}-induced synaptic membrane fusion at a concentration one order of magnitude lower than that required for IP$_6$. We further elucidated the molecular mechanism responsible for 5-IP$_7$ actions, demonstrating that 5-IP$_7$ directly bound with high affinity to synaptotagmin 1 (Syt1), a Ca^{2+} sensor in cellular exocytosis, and suppressed its fusogenic activity. Thus, our data propose 5-IP$_7$ as a potent inhibitor of Syt1 actions on Ca^{2+}-mediated synaptic vesicle fusion.

Author contributions: T.-S.L., J.-Y.L., J.W.K., Y.Y., S.H.K., T.-Y.Y., and S.K. designed research; T.-S.L., J.-Y.L., J.W.K., Y.Y., S.J.P., S.L., and B.K. performed research; I.P. and H.J.J. contributed new reagents/analytic tools; T.-S.L., J.-Y.L., J.W.K., Y.Y., Y.S.J., D.-H.K., Y.-K.S., S.H.K., T.-Y.Y., and S.K. analyzed data; and T.-S.L., J.-Y.L., Y.Y., S.H.K., T.-Y.Y., and S.K. wrote the paper.

The authors declare no conflict of interest.

This article is a PNAS Direct Submission.

[1]T.-S.L. and J.-Y.L. contributed equally to this work.

[2]To whom correspondence may be addressed. Email: sunghyunkim@khu.ac.kr, tyyoon@yonsei.ac.kr, or seyunkim@kaist.ac.kr.

This article contains supporting information online at www.pnas.org/lookup/suppl/doi:10.1073/pnas.1521600113/-/DCSupplemental.

of its function in vesicular trafficking (26, 27), we investigated the possible role of 5-IP_7 in the regulation of synaptic vesicle exocytosis at the cell and single-molecule level. Here, we report that increasing 5-IP_7 levels in PC12 cells by overexpressing IP6K1 inhibited neurotransmitter release, whereas decreasing 5-IP_7 levels by small interfering RNA (siRNA)-mediated IP6K1 knockdown stimulated neurotransmitter release. Consistently, short-hairpin RNA (shRNA)-mediated knockdown of IP6K1 in cultured hippocampal neurons augmented action potential (AP)-driven synaptic vesicle exocytosis at synapses, suggesting that 5-IP_7 is a physiologic inhibitor of synaptic vesicle exocytosis. FRET-based biophysical analyses of reconstituted synaptic vesicles further revealed that 5-IP_7 is significantly more potent in suppressing synaptic membrane fusion than other IPs, such as IP_6 and 1-IP_7. We identified Syt1 as the molecular target of 5-IP_7 actions, showing that 5-IP_7 binds to Syt1 with an affinity more than one order of magnitude higher than that of IP_6. Our present study therefore defines 5-IP_7 as a negative regulator that potently inhibits Syt1 and ultimately suppresses Ca^{2+}-evoked synaptic exocytosis.

Results

The 5-IP_7 Suppresses Neurotransmitter Release in PC12 Cells. To determine the physiological effects of 5-IP_7 in synaptic exocytosis, we first examined noradrenaline release by PC12 cells. PC12 cells, which use SNARE and Syt1 proteins for release of synaptic vesicles and large dense-core granules (28), were loaded with radioactive [^{3}H]-noradrenaline, and exocytosis was induced by treating cells with a high concentration of K^+ ions (29). Compared with control cells expressing empty vector, PC12 cells overexpressing wild-type IP6K1 (IP6K1-WT) for 48 h showed a dramatic reduction (>70%) in neurotransmitter release (Fig. S1 *A–C*). In contrast, no significant reduction in neuroexocytosis was observed upon expression of kinase-dead IP6K1 (IP6K1-KD) harboring a single K226A point mutation in the catalytic domain (Fig. S1*C*). Consistent with these observations, expression of IP6K1-WT, but not IP6K1-KD, elevated IP_7 levels within PC12 cells (Figs. S1*B* and S2). According to a previous study by Luo et al., adenoviral-mediated expression of either IP6K1-WT or -KD for 20 h causes a modest increase in dopamine release by PC12 cells (21). To understand these apparently discrepant results, we depleted IP6K1 in PC12 cells using a specific siRNA. This siRNA treatment resulted in a >90% reduction in endogenous IP6K1 protein levels, which in turn led to a ~67% decrease in cellular IP_7 levels (Figs. S1 *D* and *E* and S3). Under IP6K1-depleted conditions, neurotransmitter release was significantly increased (2.5-fold) compared with control cells treated with scrambled siRNA (Fig. S1*F*). Our results strongly suggest that 5-IP_7 acts to suppress synaptic vesicle exocytosis in PC12 cells.

Depletion of IP6K1 Potentiates Activity-Driven Synaptic Vesicle Exocytosis in Primary Hippocampal Neurons. To further verify whether depletion of IP6K1 affects synaptic vesicle release at central nervous system (CNS) synapses, we examined activity-driven exocytosis in rat primary cultured hippocampal neurons using a vGlut1-pHluorin (vGlut1-pH)–based assay combined with shRNA targeting IP6K1. When combined with a wide-field optical imaging system, this vGlut1-pH–based assay, in which the pHluorin label shows increased fluorescence upon deacidification of the vesicle lumen, has been used to monitor synaptic vesicle exocytosis at CNS synapses (30–33). We monitored vGlut1-pH responses of hippocampal neurons to 100 AP stimuli at 10 Hz, equivalent to the simultaneous monitoring of approximately 30–40 boutons of an individual neuron, in the presence or absence of shRNA against IP6K1 (sh-IP6K1). Increase in pHluorin fluorescence, which correlated with the amount of vesicle exocytosis, was measured at each synaptic bouton. We also assessed the maximum increase in pHluorin fluorescence at the corresponding bouton by stimulating its entire vesicle pool with NH_4Cl. Normalized fluorescence change (normalized ΔF) was calculated by dividing the observed fluorescence change by the maximum change observed in response to alkalization.

Normalized ΔF was significantly higher in sh-IP6K1–transfected neurons (0.32 ± 0.03) than in control neurons (0.21 ± 0.02) (Fig. 1 *A–C* and Fig. S4). Measurements of the level of expression of IP6K1 in individual neurons after live cell imaging showed that endogenous IP6K1 protein levels were significantly lower by ~70% in sh-IP6K1–transfected neurons than in control neurons (Fig. 1 *D* and *E*). Collectively, these results show that synaptic vesicle exocytosis in the IP6K1-depleted hippocampal neurons was potentiated by ~50%, suggesting that 5-IP_7 acts in a physiological setting to suppress synaptic vesicle exocytosis at CNS synapses.

Potent Inhibition of Ca^{2+}-Dependent Synaptic Vesicle Fusion by 5-IP_7. To dissect the effect of 5-IP_7 in the regulation of synaptic vesicle exocytosis, we used an in vitro vesicle fusion system that allowed monitoring of SNARE- and Syt1-mediated membrane fusion down to the single-vesicle level (34–41) (Fig. 2). In this vesicle–vesicle fusion assay, one group of vesicles (v vesicles) was reconstituted with vesicle associated membrane protein 2 (vamp2; v-SNAREs) and Syt1. The other group of vesicles (t vesicles) was reconstituted with a precomplex of t-SNARE proteins [syntaxin 1 HT and synaptosomal-associated protein 25 (SNAP-25)] stabilized by the C-terminal fragment of vamp2 (42) (Fig. S5). This set of SNARE and Syt proteins has been shown to be responsible for synaptic vesicle exocytosis in hippocampal neurons (11, 15) and PC12 cells (43). We previously reported that the fusogenic activity of membrane-anchored Syt1 can be recapitulated in vitro by providing a charge imbalance to v- and t-vesicle membranes (39). Specifically, we used 3 mol percent (mol%) phosphatidylserine (PS) lipids for the v-vesicle membrane, while adding 15 mol% PS and 1 mol% phosphatidylinositol 4,5-bisphosphate (PIP_2) for the t vesicle. Moreover, we included 1 mM Mg^{2+} ions and 1 mM ATP in the fusion reaction buffer to mimic the physiological concentrations of divalent ions and multivalent pyrophosphate molecules (41, 44). Under these conditions, fusion kinetics, measured by the mixing of lipid dyes that constitute a FRET donor and acceptor pair [1,1′-dioctadecyl-3,3,3′,3′-tetramethylindocarbocyanine perchlorate (DiI) and 1,1′-dioctadecyl-3,3,3′,3′-tetramethylindodicarbocyanine perchlorate (DiD)], was significantly accelerated at a Ca^{2+} concentration of 100 μM (Fig. S6). Because this Ca^{2+}-evoked acceleration of vesicle–vesicle fusion was observed in a bulk assay setting, we reasoned that a majority of vesicle–vesicle fusion events, rather than that of a small subset of vesicles, was accelerated.

Addition of IP_6 or IP_7 to the fusion reaction buffer caused a marked inhibition of SNARE- and Syt1-mediated membrane fusion (Fig. 2 *A* and *B*). Remarkably, 5-IP_7 was 10-fold more potent in inhibiting membrane fusion than IP_6 (Fig. 2*C*). As a measure of fusion activity, we compared fluorescence changes at 5 min after initiation of fusion by mixing of t and v vesicles. Whereas 429 μM IP_6 was needed to decrease the fusion activity by 50% (i.e., IC_{50} value), 44 μM 5-IP_7 was sufficient to achieve the same level of suppression (Fig. 2*C*). Similar potent inhibition was not detected with 1-IP_7 or other IPs [e.g., inositol 1,3,4,5-tetrakisphosphate (IP_4) or inositol 1,3,4,5,6-pentakisphosphate (IP_5)], indicating the specificity of the 5-IP_7 effect (Fig. 2*C* and Fig. S7).

We further examined the inhibitory effect of 5-IP_7 on fusion at the single-vesicle level. Single vesicle–vesicle docking kinetics were monitored by immobilizing 30,000 v vesicles in an imaging area of 45 × 90 μm^2 and reacting them with 0.1 μM t vesicles (Fig. S8). After reacting for 30 s, the single-vesicle docking number (i.e., number of docked t vesicles for each imaging area), which we assumed was proportional to the kinetic rate of docking between v and t vesicles, was quantified. The addition of 5-IP_7 led to a significant reduction in the single-vesicle docking number, an effect that was evident at low micromolar concentrations (Fig. 2*D*). Only 3.7 μM 5-IP_7 was required for 50% inhibition in the single-vesicle docking assay (Fig. 2*E*), a value one order of magnitude lower than

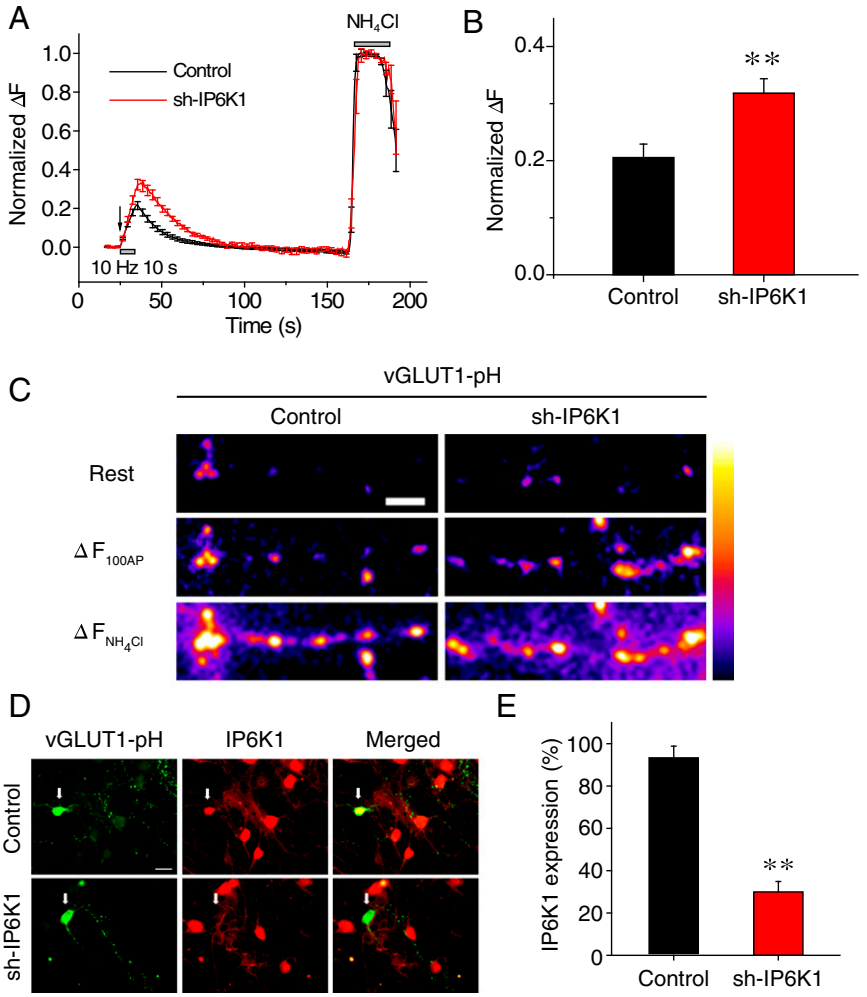

Fig. 1. Depletion of IP6K1 increases activity-driven synaptic vesicle exocytosis at CNS synapses. (*A*) Ensemble-averaged traces of vGlut1-pH response to 100 AP stimuli and NH_4Cl application from control (17 cells, 726 boutons) and sh-IP6K1–transfected (18 cells, 667 boutons) neurons. Transfected hippocampal neurons were stimulated by 100 AP at 10 Hz, followed by NH_4Cl application. Intensities were normalized to the peak value of NH_4Cl response (total vesicle pool). The arrow indicates the point of stimulation. Error bars represent SEs. (*B*) Mean amplitudes of 100 AP responses (amount of vesicle release) from control (20.55% ± 2.38%; 17 cells, 726 boutons) and sh-IP6K1–transfected (31.80% ± 2.57%; 18 cells, 667 boutons) neurons. Results represent the mean of six independent primary cultures. Approximately 30–40 responsive synaptic boutons per neuron were measured. (*C*) Representative fields of vGlut1-pH fluorescence images at rest, a difference image for 100 AP (ΔF_{100AP}) and during NH_4Cl application to control and sh-IP6K1–transfected neurons. (Scale bar, 5 μm.) (*D*) Representative images of hippocampal neurons double-stained with anti-GFP (green) and anti-IP6K1 (red) antibodies. After live cell imaging, the neurons were fixed and stained with anti-GFP and -IP6K1 antibodies. Arrows indicate transfected neurons in each condition. (Scale bar, 10 μm.) (*E*) Mean IP6K1 expression in control and sh-IP6K1 neurons. $[IP6K1]_{con}$ = 92.51% ± 6.42%; $[IP6K1]_{sh\text{-}IP6K1}$ = 29.98% ± 4.89%. Results represent 17 control and 14 sh-IP6K1 cells from six independent primary cultures. Error bars represent mean ± SEM. $^{**}P < 0.01$ (Student's *t* test).

the IC_{50} value measured for the bulk fusion assay (44 μM) (Fig. 2*C*). This IC_{50} value was approximately one order of magnitude lower than that measured for inhibition of single-vesicle docking by IP_6, 1-IP_7, or other IPs (e.g., IP_4 or IP_5) (Fig. 2*E* and Fig. S9). Our data imply that the inhibitory effect of 5-IP_7 is more critical for a subset of vesicles with higher fusion activities, because the single-vesicle assay selectively monitors higher-activity vesicles (i.e., those that react within the given 30-s time window). Our observations indicate that 5-IP_7 at tens of micromolar concentrations exhibits a significant inhibitory effect in the presence of 1 mM ATP, which is also a pyrophosphate molecule (41). Therefore, it appears that the inhibitory effect of 5-IP_7 does not arise from simple electrostatic screening. Instead, 5-IP_7 may regulate one of the components in the minimal vesicle fusion system consisting of lipid molecules, SNAREs, and Syt1 (see below).

The 5-IP_7 Inhibits Synaptic Vesicle Fusion by Targeting Syt1. Next, we examined the molecular target of 5-IP_7 using our in vitro fusion system. First, we removed the SNARE proteins from our fusion assay. Protein-free t vesicles were reacted with v vesicles that were reconstituted with only Syt1. We observed inhibition of vesicle–vesicle fusion in a 5-IP_7–dependent manner (Fig. 3*A*). In contrast, removal of Syt1 from the fusion system nearly abolished the inhibitory effect of 5-IP_7 in the concentration range studied (Fig. 3*B*). These observations suggest that 5-IP_7 exerts its inhibitory effects on synaptic vesicle fusion by targeting Syt1.

It has been reported that various IPs, including IP_6, bind to the C2AB domain of Syt1 (16–20, 45), which is known to play a crucial role in sensing Ca^{2+} ions as well as mediating synaptic membrane fusion (46). We thus examined binding kinetics of 5-IP_7 and IP_6 to the C2AB domain using surface plasmon resonance (SPR) spectroscopy. To our surprise, the concentration of 5-IP_7 required to obtain a given level of response was 45-fold smaller than that of IP_6 (Fig. 3 *C*–*E*). These SPR data likely indicate that the affinity of 5-IP_7 for Syt1–C2AB binding is enhanced to the same degree, also

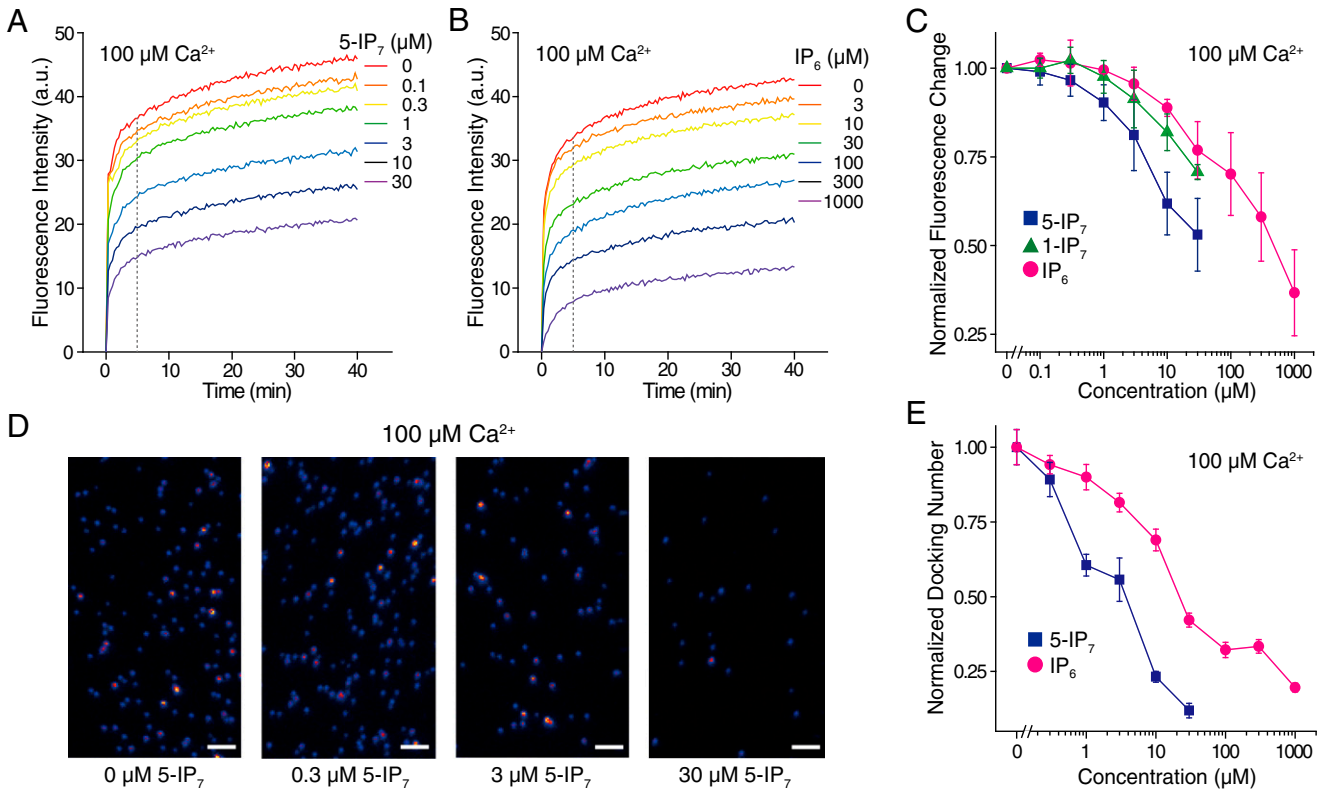

Fig. 2. The 5-IP_7 suppresses Ca^{2+}-dependent vesicle fusion in vitro. (*A* and *B*) Lipid mixing of t and v vesicles was traced in the presence of 5-IP_7 (*A*) or IP_6 (*B*) in the presence of 100 μM Ca^{2+}. The *y* axis is acceptor fluorescence intensity produced by FRET between the donor and acceptor dyes in vesicles, a measure of the activity of vesicle fusion with lipid mixing. (*C*) Plot of the normalized fluorescence change at 5 min for 5-IP_7 (*A*) or IP_6 (*B*), and 1-IP_7. (*D*) Exemplary images of single-vesicle docking assays in the presence of 5-IP_7. (Scale bars, 3 μm.) (*E*) Quantification of data from *D*. Error bars represent SD.

consistent with the higher efficacy of 5-IP_7 in suppressing in vitro vesicle fusion compared with IP_6, as shown in Fig. 2. One more noteworthy observation was that the SPR data showed near-instantaneous increases and decreases in response units upon addition and removal of 5-IP_7, IP_6, and Ca^{2+} (Fig. 3 *C*–*E* and Fig. S10). These observations indicate that binding and unbinding of these small molecules to the Syt1–C2AB domain are fast kinetic processes that cannot be resolved with the time scale of our SPR assay (1 s).

To investigate whether 5-IP_7 acts through Syt1 C2 domains under physiological conditions, we revisited the cell-based noradrenaline release assay shown in Fig. S1, with the difference that PC12 cells were cotransfected with the IP6K1-WT and GST-tagged Syt1–C2B domain (Fig. S11*A*). IP6K1-dependent inhibition of noradrenaline release was significantly rescued by the expression of Syt1–C2B (Fig. S11*B*). This result suggests that excess Syt1–C2B domains adsorbed 5-IP_7, making less 5-IP_7 available for binding to endogenous Syt1, which had the net effect of reactivating the release process. These results collectively indicate that 5-IP_7 suppresses vesicle fusion through interactions with the Syt1–C2AB domain.

Finally, we sought to characterize the molecular interactions of Syt1 with its two ligands, Ca^{2+} and 5-IP_7. We initially performed in vitro vesicle fusion assays under Ca^{2+}-chelated conditions. With 5 μM EGTA in the reaction buffer, we observed that 5-IP_7 still exerted a potent, concentration-dependent inhibitory effect on vesicle fusion (Fig. 3*F*). This observation indicates that the inhibitory effect of 5-IP_7 does not result from simple inhibition of Ca^{2+} binding to Syt1. Instead, 5-IP_7 likely exerts its inhibitory effect through a binding region in C2AB that is independent of the Ca^{2+}-binding region. Moreover, our in vitro fusion assay showed that, as the Ca^{2+} level was increased in the vesicle fusion assay, the concentration of 5-IP_7 needed to obtain the same level of inhibition concomitantly increased (Fig. 3 *G* and *H*), suggesting that the inhibitory effect of 5-IP_7 can be overcome by excess Ca^{2+} ions.

Discussion

Despite the fundamental importance of IPs in various vesicle trafficking events, there is as yet no consensus on the functional significance of IP_7 in the control of synaptic vesicle exocytosis. To resolve this important issue, we used a combination of cell biology, biochemistry, and single-vesicle biophysical assays. These analyses provide several lines of evidence to show that 5-IP_7 inhibits synaptic vesicle fusion through direct interaction with Syt1. (*i*) Increasing in IP_7 in PC12 cells by overexpressing IP6K1-WT suppressed noradrenaline release, whereas overexpressing catalytically inactive IP6K1 had no such effect. Conversely, decreasing IP_7 in PC12 cells by specific depletion of IP6K1 significantly increased depolarization-induced noradrenaline release. (*ii*) Knockdown of IP6K1 in primary cultured hippocampal neurons potentiated AP-driven synaptic vesicle exocytosis. (*iii*) FRET-based, single-molecule imaging of biochemically reconstituted synaptic vesicles showed that 5-IP_7 exhibited a 10-fold higher efficiency in inhibiting vesicle fusion process compared with IP_6 and 1-IP_7. This 5-IP_7 action was detected only when Syt1 was present in the assay system. (*iv*) SPR-based, small molecule-protein binding assays revealed a direct interaction between 5-IP_7 and Syt1. The Syt1–C2AB domain was found to display a 45-fold higher binding affinity for 5-IP_7 than for IP_6. (*v*) Finally, exogenously supplied Syt1–C2B abolished IP6K1-dependent inhibition of neurotransmitter release in PC12 cells.

In particular, our results strongly point to dynamic, negative regulation of Syt1 activity by 5-IP_7. Through binding to the C2AB domain, 5-IP_7 appears to restrain Syt1 in a functionally incompetent conformation. Our observation that 5-IP_7 inhibited vesicle fusion even under Ca^{2+}-chelated conditions suggests that it is unlikely that

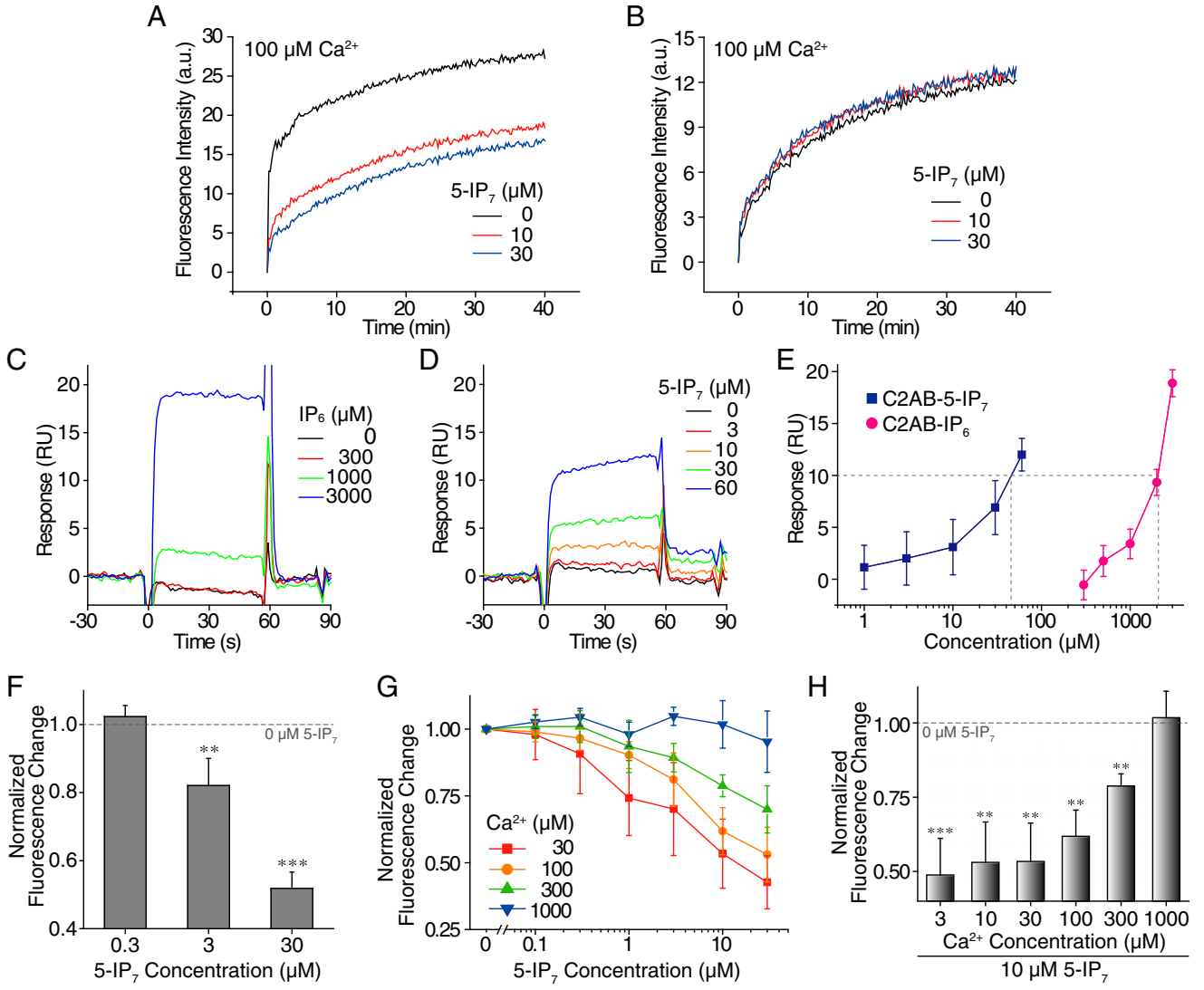

Fig. 3. The 5-IP$_7$ inhibits synaptic vesicle fusion via Syt1. (*A* and *B*) The effect of 5-IP$_7$ on lipid mixing of t and v vesicles was measured by preparing t vesicles without SNARE (*A*). Syt1 in v vesicles was the only protein component in this vesicle fusion assay. In *B*, v vesicles were prepared without Syt1 proteins. (*C*–*E*) The 5-IP$_7$ (*C*) and IP$_6$ (*D*), as analytes, were applied to the purified Syt1–C2AB domain immobilized on a sensor chip. Syt1-binding data are summarized for 5-IP$_7$ and IP$_6$, showing their different binding affinities (*E*). (*F*) The effect of 5-IP$_7$ on vesicle fusion was measured under Ca^{2+}-free, 5 μM EGTA conditions. (*G* and *H*) Lipid mixing observed in the presence of 5-IP$_7$ and Ca^{2+} at various concentrations (*G*). Data for 10 μM 5-IP$_7$ conditions are presented as a plot of normalized fluorescence intensity as a function of Ca^{2+} concentration (*H*). Error bars represent SD. ***$P < 0.001$; **$P < 0.01$ [one-sample *t* test (*F* and *H*)].

the inhibitory effect of 5-IP$_7$ results from hindering Ca^{2+} binding to Syt1. Conversely, we found that Ca^{2+} in excess steered Syt1 toward a fusion-competent conformation. Together, these observations suggest that, although 5-IP$_7$ and Ca^{2+} do not directly compete with each other for Syt1 binding, their relation at the functional level is effectively competitive. In addition, our SPR assays suggest that the binding and unbinding kinetics of Ca^{2+} and IP$_7$ (and IP$_6$) for Syt1 are very rapid. Thus, we hypothesize that Syt1 is in a dynamic equilibrium between fusion-competent and -incompetent conformations, with the balance between them being delicately shifted as Ca^{2+} and 5-IP$_7$ levels are physiologically altered.

The functional interaction between 5-IP$_7$ and Syt1 uncovered in this study suggests a role for 5-IP$_7$ in controlling the exocytosis process. Intracellular 5-IP$_7$ concentrations are in the low micromolar range and show extremely rapid and dynamic turnover (9, 22–25), consistent with our conclusion that 5-IP$_7$ functions as a molecular switch for synaptic exocytosis. We speculate that IP6K1 and its product 5-IP$_7$ may exert multiple modes of regulation at different levels. On one level, 5-IP$_7$, the product of IP6K1, can act as a negative regulator of Syt1, thus inhibiting synaptic vesicle fusion. On another level, as previously proposed (21), IP6K1 can directly bind to GRAB in a noncatalytic manner, which facilitates early steps of vesicle docking. Further studies will be needed to elucidate full details of the complex relationship between 5-IP$_7$–Syt1 signaling and the IP6K1–GRAB pathway. It would also be interesting to test whether the activity of 5-IP$_7$ depends on cell type-specific Syt isoforms. Whereas 5-IP$_7$ functions as a Syt1 inhibitor in neuronal cells, 5-IP$_7$ may promote insulin exocytosis in the pancreas, where beta cells express the Syt3 isoform, but not Syt1 (27).

Finally, an imbalance in IP levels in the human body, as well as genetic deletion of IP6K enzymes in mouse models, has been implicated in a number of psychiatric and neurodegenerative diseases (47–50). It will be important to gain insights into the structural mechanism underlying high-affinity 5-IP$_7$ binding and inhibition of the Syt1 protein. We expect that the unique binding of 5-IP$_7$ to Syt1 can be used to guide the design of small molecules that have therapeutic potential to allosterically control the release of neurotransmitters.

Materials and Methods

The 5- and 1-IP_7 were synthesized (Fig. S12) as previously described (51, 52). In vitro bulk-vesicle fusion and single-vesicle docking assays were performed as described previously (39). Reagents and all experimental procedures, such as SPR analysis and pHluorin-based assay in cultured hippocampal neurons, are fully described in *SI Materials and Methods*.

ACKNOWLEDGMENTS. We thank Eunji Kim, Ji-Joon Song, and all the members of the T.-Y.Y. and S.K. laboratories for discussion and helpful comments. This work was supported by the National Creative Research Initiative Program Center for Single-Molecule Systems Biology (T.-Y.Y); Institute for Basic Science Grant IBS-R0216-D1; and National Research Foundation of Korea Grants NRF-2013R1A1A1063174 (to S.H.K.) and NRF-2013M3C7A1056102 (to S.K.).

1. Irvine RF, Schell MJ (2001) Back in the water: The return of the inositol phosphates. *Nat Rev Mol Cell Biol* 2(5):327–338.
2. Barker CJ, Illies C, Gaboardi GC, Berggren PO (2009) Inositol pyrophosphates: Structure, enzymology and function. *Cell Mol Life Sci* 66(24):3851–3871.
3. Hatch AJ, York JD (2010) SnapShot: Inositol phosphates. *Cell* 143(6):1030–1030.e1.
4. Mulugu S, et al. (2007) A conserved family of enzymes that phosphorylate inositol hexakisphosphate. *Science* 316(5821):106–109.
5. Lee YS, Mulugu S, York JD, O'Shea EK (2007) Regulation of a cyclin-CDK-CDK inhibitor complex by inositol pyrophosphates. *Science* 316(5821):109–112.
6. Chakraborty A, et al. (2010) Inositol pyrophosphates inhibit Akt signaling, thereby regulating insulin sensitivity and weight gain. *Cell* 143(6):897–910.
7. Szijgyarto Z, Garedew A, Azevedo C, Saiardi A (2011) Influence of inositol pyrophosphates on cellular energy dynamics. *Science* 334(6057):802–805.
8. Saiardi A, Bhandari R, Resnick AC, Snowman AM, Snyder SH (2004) Phosphorylation of proteins by inositol pyrophosphates. *Science* 306(5704):2101–2105.
9. Chakraborty A, Kim S, Snyder SH (2011) Inositol pyrophosphates as mammalian cell signals. *Sci Signal* 4(188):re1.
10. Rothman JE (1994) Mechanisms of intracellular protein transport. *Nature* 372(6501):55–63.
11. Sudhof TC (2004) The synaptic vesicle cycle. *Annu Rev Neurosci* 27:509–547.
12. Jahn R, Scheller RH (2006) SNAREs—Engines for membrane fusion. *Nat Rev Mol Cell Biol* 7(9):631–643.
13. Chapman ER (2008) How does synaptotagmin trigger neurotransmitter release? *Annu Rev Biochem* 77:615–641.
14. Rizo J, Rosenmund C (2008) Synaptic vesicle fusion. *Nat Struct Mol Biol* 15(7):665–674.
15. Jahn R, Fasshauer D (2012) Molecular machines governing exocytosis of synaptic vesicles. *Nature* 490(7419):201–207.
16. Fukuda M, Aruga J, Niinobe M, Aimoto S, Mikoshiba K (1994) Inositol-1,3,4,5-tetrakisphosphate binding to C2B domain of IP4BP/synaptotagmin II. *J Biol Chem* 269(46):29206–29211.
17. Llinás R, et al. (1994) The inositol high-polyphosphate series blocks synaptic transmission by preventing vesicular fusion: A squid giant synapse study. *Proc Natl Acad Sci USA* 91(26):12990–12993.
18. Fukuda M, et al. (1995) Role of the C2B domain of synaptotagmin in vesicular release and recycling as determined by specific antibody injection into the squid giant synapse preterminal. *Proc Natl Acad Sci USA* 92(23):10708–10712.
19. Sasakawa N, et al. (2011) Dissociation of inositol polyphosphates from the C2B domain of synaptotagmin facilitates spontaneous release of catecholamines in adrenal chromaffin cells. A suggestive evidence of a fusion clamp by synaptotagmin. *Neuropharmacology* 60(7-8):1364–1370.
20. Yang SN, et al. (2012) Inositol hexakisphosphate suppresses excitatory neurotransmission via synaptotagmin-1 C2B domain in the hippocampal neuron. *Proc Natl Acad Sci USA* 109(30):12183–12188.
21. Luo HR, et al. (2001) GRAB: A physiologic guanine nucleotide exchange factor for Rab3A, which interacts with inositol hexakisphosphate kinase. *Neuron* 31(3):439–451.
22. Glennon MC, Shears SB (1993) Turnover of inositol pentakisphosphates, inositol hexakisphosphate and diphosphoinositol polyphosphates in primary cultured hepatocytes. *Biochem J* 293(Pt 2):583–590.
23. Albert C, et al. (1997) Biological variability in the structures of diphosphoinositol polyphosphates in *Dictyostelium discoideum* and mammalian cells. *Biochem J* 327(Pt 2):553–560.
24. Tsui MM, York JD (2010) Roles of inositol phosphates and inositol pyrophosphates in development, cell signaling and nuclear processes. *Adv Enzyme Regul* 50(1):324–337.
25. Shears SB, Weaver JD, Wang H (2013) Structural insight into inositol pyrophosphate turnover. *Adv Biol Regul* 53(1):19–27.
26. Saiardi A, Sciambi C, McCaffery JM, Wendland B, Snyder SH (2002) Inositol pyrophosphates regulate endocytic trafficking. *Proc Natl Acad Sci USA* 99(22):14206–14211.
27. Illies C, et al. (2007) Requirement of inositol pyrophosphates for full exocytotic capacity in pancreatic beta cells. *Science* 318(5854):1299–1302.
28. Westerink RH, Ewing AG (2008) The PC12 cell as model for neurosecretion. *Acta Physiol (Oxf)* 192(2):273–285.
29. Ray P, Berman JD, Middleton W, Brendle J (1993) Botulinum toxin inhibits arachidonic acid release associated with acetylcholine release from PC12 cells. *J Biol Chem* 268(15):11057–11064.
30. Miesenböck G, De Angelis DA, Rothman JE (1998) Visualizing secretion and synaptic transmission with pH-sensitive green fluorescent proteins. *Nature* 394(6689):192–195.
31. Kim SH, Ryan TA (2010) CDK5 serves as a major control point in neurotransmitter release. *Neuron* 67(5):797–809.
32. Kim SH, Ryan TA (2013) Balance of calcineurin Aα and CDK5 activities sets release probability at nerve terminals. *J Neurosci* 33(21):8937–8950.
33. Hoppa MB, Gouzer G, Armbruster M, Ryan TA (2014) Control and plasticity of the presynaptic action potential waveform at small CNS nerve terminals. *Neuron* 84(4):778–789.
34. Weber T, et al. (1998) SNAREpins: Minimal machinery for membrane fusion. *Cell* 92(6):759–772.
35. Tucker WC, Weber T, Chapman ER (2004) Reconstitution of Ca2+-regulated membrane fusion by synaptotagmin and SNAREs. *Science* 304(5669):435–438.
36. Araç D, et al. (2006) Close membrane-membrane proximity induced by Ca(2+)-dependent multivalent binding of synaptotagmin-1 to phospholipids. *Nat Struct Mol Biol* 13(3):209–217.
37. Martens S, Kozlov MM, McMahon HT (2007) How synaptotagmin promotes membrane fusion. *Science* 316(5828):1205–1208.
38. Stein A, Radhakrishnan A, Riedel D, Fasshauer D, Jahn R (2007) Synaptotagmin activates membrane fusion through a Ca2+-dependent trans interaction with phospholipids. *Nat Struct Mol Biol* 14(10):904–911.
39. Lee HK, et al. (2010) Dynamic Ca2+-dependent stimulation of vesicle fusion by membrane-anchored synaptotagmin 1. *Science* 328(5979):760–763.
40. Kyoung M, et al. (2011) In vitro system capable of differentiating fast Ca2+-triggered content mixing from lipid exchange for mechanistic studies of neurotransmitter release. *Proc Natl Acad Sci USA* 108(29):E304–E313.
41. Park Y, et al. (2012) Controlling synaptotagmin activity by electrostatic screening. *Nat Struct Mol Biol* 19(10):991–997.
42. Pobbati AV, Stein A, Fasshauer D (2006) N- to C-terminal SNARE complex assembly promotes rapid membrane fusion. *Science* 313(5787):673–676.
43. Greene LA, Tischler AS (1976) Establishment of a noradrenergic clonal line of rat adrenal pheochromocytoma cells which respond to nerve growth factor. *Proc Natl Acad Sci USA* 73(7):2424–2428.
44. Torres J, et al. (2005) Solution behaviour of myo-inositol hexakisphosphate in the presence of multivalent cations. Prediction of a neutral pentamagnesium species under cytosolic/nuclear conditions. *J Inorg Biochem* 99(3):828–840.
45. Joung MJ, Mohan SK, Yu C (2012) Molecular level interaction of inositol hexaphosphate with the C2B domain of human synaptotagmin I. *Biochemistry* 51(17):3675–3683.
46. Mackler JM, Drummond JA, Loewen CA, Robinson IM, Reist NE (2002) The C(2)B Ca(2+)-binding motif of synaptotagmin is required for synaptic transmission in vivo. *Nature* 418(6895):340–344.
47. Belmaker RH, Bersudsky Y, Agam G, Levine J, Kofman O (1996) How does lithium work on manic depression? Clinical and psychological correlates of the inositol theory. *Annu Rev Med* 47:47–56.
48. Nagata E, et al. (2011) Inositol hexakisphosphate kinases induce cell death in Huntington disease. *J Biol Chem* 286(30):26680–26686.
49. Chakraborty A, Latapy C, Xu J, Snyder SH, Beaulieu JM (2014) Inositol hexakisphosphate kinase-1 regulates behavioral responses via GSK3 signaling pathways. *Mol Psychiatry* 19(3):284–293.
50. Fu C, et al. (2015) Inositol hexakisphosphate kinase-3 regulates the morphology and synapse formation of cerebellar purkinje cells via spectrin/adducin. *J Neurosci* 35(31):11056–11067.
51. Capolicchio S, Thakor DT, Linden A, Jessen HJ (2013) Synthesis of unsymmetric diphospho-inositol polyphosphates. *Angew Chem Int Ed Engl* 52(27):6912–6916.
52. Capolicchio S, Wang H, Thakor DT, Shears SB, Jessen HJ (2014) Synthesis of densely phosphorylated bis-1,5-diphospho-myo-inositol tetrakisphosphate and its enantiomer by bidirectional P-anhydride formation. *Angew Chem Int Ed Engl* 53(36):9508–9511.
53. Tsai RY, Reed RR (1997) Using a eukaryotic GST fusion vector for proteins difficult to express in *E. coli*. *Biotechniques* 23(5):794–796, 798, 800.
54. Kim S, et al. (2011) Amino acid signaling to mTOR mediated by inositol polyphosphate multikinase. *Cell Metab* 13(2):215–221.
55. Loss O, Azevedo C, Szijgyarto Z, Bosch D, Saiardi A (2011) Preparation of quality inositol pyrophosphates. *J Vis Exp* (55):e3027.